




Synthesis of folic acid functionalized, tannic acid-based gold quantum dots for potential use in various applications

Kartikey J. Chavan^{1,2}, Sarang R. Bhagwat¹, Gayatri M. Gaidhane¹, Bhimmarao M. Patil³, Taeyeob Kim⁴, Hansol Kang⁵, Arpita Pandey Tiwari⁶, Insik In^{5,*}, Ravindra N. Bulakhe^{4,*} , and Ji Man Kim^{4,*}

¹Rayat Shikshan Sanstha's Karmaveer Bhaurao Patil College Vashi, Navi Mumbai, India

²School of Medical Science, Faculty of Biology, Medicine and Health, University of Manchester, Manchester, UK

³Institute of Science, HBSU, Fort, Mumbai, India

⁴Department of Chemistry, Sungkyunkwan University, Suwon 16419, Republic of Korea

⁵Department of Polymer Science and Engineering, Korea National University of Transportation, Chungju 380-702, South Korea

⁶Department of Medical Biotechnology, Centre for Interdisciplinary Research, D.Y. Patil Education Society (Deemed to Be University), Kolhapur, India

Received: 31 May 2023

Accepted: 16 October 2023

Published online:

7 November 2023

© The Author(s), under exclusive licence to Springer Science+Business Media, LLC, part of Springer Nature, 2023

ABSTRACT

Surface modification of gold quantum dots (AuQDs) has emerged as a highly interesting area of study in terms of different applications, such as sensors, medical, and aerospace technology. For synthesis of gold quantum dots (AuQDs) nucleation, growth, and stability is most important factor. To control nucleation, growth, and stability, monodispersed spherical AuQDs were synthesized using sodium citrate and tannic acid. PEG 6000 was then used to coat these AuQDs. The FA was conjugated with PEG-AuQDs to form nanoconjugates known as FA-PEG-AuQDs using N-ethyl-N'-(3-(dimethylamino)propyl) carbodiimide (EDC)/N-hydroxysuccinimide (NHS) coupling procedure. XPS, TEM, HR-TEM and other techniques were used to characterize AuQDs and FA-PEG-AuQDs.

1 Introduction

Nowadays, there has been improvement in the field of nanotechnology where intriguing findings have opened up new possibilities in aerospace technology, electronic technology to cure cancer by targeting and detecting cancer cells [1]. In the field of nano-technology, gold nanoparticles are known for their biologically relevant sized, low toxicities, high surface areas, ease to functionalize with biomolecules, and

well-defined optical properties that can be used to modify imaging, aero science, and therapeutic delivery. Due to these characteristics, gold nanoparticles have gained attention of the scientific community of nanotechnology for vast applications in various field among which there is use of QDs as a drug delivery vesicle, previously ZnS, Carbon QDs have been effectively used due to properties, like highly improved surface area and ability to carry water insoluble drugs

Address correspondence to E-mail: in1@ut.ac.kr; bulakhe@skku.edu; jimankim@skku.edu

to the target with optimum concentration of the drug [2, 3].

Numerous drug delivery vehicle systems based on folate have been created or enhanced to transport drugs is also one kind of use of quantum dots. [4, 5]. Polycaprolactone and hyperbranched polyester modified with L-lysine are examples of biodegradable materials based on polymers. Polymer-based materials has been a leading solicitude in relation to incarnation of integrated carriers for drugs. Recently, metal nanoparticles such as silver, platinum, and gold are extensively used in medical field due to their ability to form specific morphology which includes size and other dimensions that could ease surface functionalization with biomolecules [6].

The FA receptor, which is more prevalent on damaged or affected cells compared to normal cells, can be utilized to facilitate targeted drug delivery to these affected cells. [7]. FA can be vastly attached with different NPs as well as polymers which are biocompatible and can act as a targeting moiety. Therefore, FA-functionalized Au QDs have been immensely studied for their drug delivery activities.

FA-functionalized AuQDs have been developed by Shakeri-Zadeh et al. [8] using linking agents such as p-aminothiophenol and 6-mercaptohexanol. To develop adequate platforms of AuNP nanoconjugate that are FA-based, two formulation parameters are crucial: (1) conjugation of polymeric compounds to achieve colloidal stability of nanoparticles and (2) bonding of FA covalently to PEG-conjugated AuNPs [9, 10].

The production of biocompatible Au QDs has been achieved through the use of green synthesis methods, which involve the utilization of solvents like water and biomolecules, such as phytochemicals as reducing and stabilizing agents. Synthetic polymers and bifunctional copolymers like citrate-PEG (CPEG) are commonly employed as both reducing and stabilizing agents in the production of AuNPs. [11, 12]. Because of its qualities, such as electrical neutrality and high hydrophilicity, PEG is frequently used for applications like grafting and adsorption to surfaces of NPs.

After the NPs have been PEGylated, a protective hydrophilic coating forms around them which serves as a bridge to link ligands or peptides that are tailored to its hydroxy terminus, which can bind to the surface of cells containing specific receptors, also known as

targeted delivery. PEG, which possesses a wide range of capabilities include increasing the delivery of specific NPs, preventing the removal of NPs by the MPS and adapting some physicochemical features, such as the mechanical properties of membrane and behavior of drug loading and release [13].

Bifunctional polyphenol-based polymers can serve as both reducing and stabilizing agents in the synthesis of Au QDs, as well as linkers for attaching FA (folic acid) via covalent bonds [14, 15]. Basically, Tannins are compounds which are phenolic and resulting from several plants having high ecological values. Its benefits are widely expressed by TA, including antioxidant, anticancer, neuroprotective, and anti-inflammatory properties [16]. Tannic acid contains a link that is hydroxyl, which boost water solubility [17]. The capacity to interact with macromolecules and biopolymers through cross-linking makes TA a prospective medicinal candidate. This is because of its hydroxy and carboxy groups. Thanks to its potential polyphenolic phytochemicals, TA plays a significant role in synthesis of quantum dots demonstrating anti-tumorigenic effects [18]. Tannic acid (TA) is a type of polyphenol with a structure that allows for strong binding with various species through hydrophobic, multiple hydrogen bonding, π - π , and cation- π interactions.

Some naturally occurring polyphenols, such as TA and EGCG, have been shown to exhibit endocytosis behavior [19]. Additionally, polyphenol molecules and nanoparticles can interact with biomolecules, such as proteins, nucleic acids, and phospholipids, through several non-covalent interactions, which can be useful for gene delivery and cell coating [20]. In the recent years, the application of TA in primary chemoprevention as well as sensitization to conventional drugs are used in therapy for carcinogenesis [21]. Coordination reactions can be used to create metal-phenolic cross-linking networks, hydrogels, nanoparticles, and coatings [22].

Therefore, in the present study, PEG-coated quantum dots were surface functionalized with tannic acid. Tannic acid was used as a reducer and a stabilizer for the synthesis of gold nanoparticles. Folic acid was then attached to the -AuQDs group via polyphenol by the reaction of carbodiimide coupling, resulting in FA-PEG-TA-AuQDs. As size increased due to the addition of FA, quantum dots changed into nanoparticles. The morphological and

structural characteristics of FA-PEG-TA-AuQD were then determined.

2 Materials and methods

2.1 Materials

Tannic acid (Sd Fine Chem Ltd, India), sodium citrate (Loba Chemie Pvt Ltd, India), stannous chloride dehydrate (Loba Chemie Pvt Ltd, India), potassium carbonate (Loba Chemie Pvt Ltd, India), PEG6000 (Merck Life Science Pvt. Ltd), gold (III) chloride hydrate (ultrapure 99.99%, ~ 49% Au) (Sisco Research Laboratories Pvt. Ltd.), 1,2-dichloroethane or ethylene dichloride (EDC) (Sd Fine Chem Ltd, India), 1-hydroxysuccinimide (NHS) (Sd Fine Chem Ltd, India), and folic acid Sd Fine Chem Ltd, India) were procured.

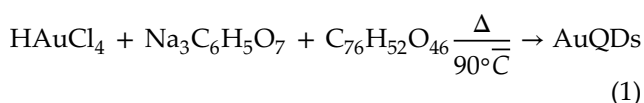
2.2 Characterization techniques

Transmission electron microscope images were obtained on TECNAI 120 kV d1240 Bio Twin. High-Resolution Transmission Electron Microscopy (HR-TEM) system images were captured on JEOL JEM 2100 at 200 keV. PEG-TA- AuQDs [AuQDs with PEG 6000] were equally laid on small pieces of glass slide. XPS spectra of samples were recorded on (Omicron ESCA, Oxford Instrument, Germany) instrument. FTIR spectrometer spectrums were recorded using a PerkinElmer Spectra Version 10.03.07. EDAX analysis was carried on by EVO-18 scanning electron microscope (Carl Zeiss, Germany). UV spectroscopy of FA-PEG-TA-AuQDs was run at 200–700 nm UV–vis range on Shimadzu-1800 spectrophotometer.

2.3 Synthesis of tannic acid-based gold quantum dots (TA-Au QDs)

Tannic acid (TA) significantly altered the kinetics of Au NP synthesis when it is added to the method named Inverse Turkevich [23] resulting in rapid and regular generation of 3.3 nm Gold NPs. Simply stated by chemical reduction of the gold precursor HAuCl_4 by dissolved trisodium citrate at 90 °C from

aqueous solutions containing (HAuCl_4 0.20 mM) and (SC, 2.1 mM, 150 mL) of gold precursor and citrate, respectively. Along with the addition of tannic acid (TA, 2 mM, 0.1 mL) which acts as a strong reducing agent producing narrowly dispersed gold quantum dots. Above mechanism is presented in the reaction. In order to get size maintained AuQDs add 1 ml of potassium carbonate (K_2CO_3 , 150 Mm, 1mL) leading to synthesis of small size AuQDs compared to the other pH factors as shown in earlier studies. And in order to attach the FA [24] and while using [EDC/NHS] as loading agent, no pH change was observed and hence no optimization was carried out [24].

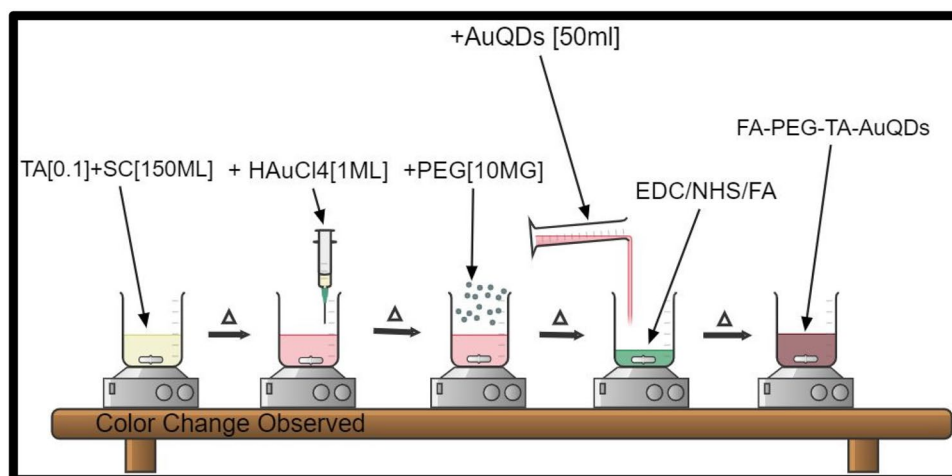


After injecting the gold precursor, the solution changed from translucent to blackish gray instantly. After a few minutes, it turned in to crimson color, indicating the creation of tiny Au QDs. Use of TA at low quantity and having reducing power comparatively more than SC appeared to be essential. The use of TA in low quantity which has a reducing power appearing to be higher than SC which is responsible for the critical formation of smaller nano particles [25]. As SC is also the reducer, addition of TA increases the reducing power As both reducers are necessary, their absence could result in polydisperse and large particles. After the synthesis, the solution was kept in dark condition. The schematic of the detailed synthesis procedure is provided in above scheme 1.

2.4 Coating of PEG -6000 to tannic acid-based gold quantum dot (PEG-TA-AuQD)

Tannic acid-based gold quantum dots were dissolved in PEG 6000 (10 mg) and the reaction was carried out at 90 °C for 12 h under normal atmospheric conditions before being cooled to ambient temperature. After the attachment of PEG 6000 the solution of PEG-TA-AuQDs was placed in dark condition.

Scheme 1 The detailed synthesis procedure of Au NPs



2.5 Attachment of folic acid to PEG-TA-AuQDs (FA-PEG-TA-AuQDs)

One-pot synthesis of synthesis of FA-PEG-TA-AuQDs and drug loading onto it was carried out using modified method of Gajendiran et al. [26]. Separate solutions of NHS [2.5 mM], EDC [2.5 mM], and FA [2.5 mM] were prepared. 50 ml of PEG-TA-AuQDs solution was mixed with equimolar ratio of EDC and NHS in a flask which was maintained at room temperature away from sunlight on magnetic stirrer. To this mixture, FA was added with the flow rate of 5 ml/min and stirring was continued overnight.

The obtained solution then was used for characterization.

3 Results and discussion

3.1 Morphological properties of tannic acid-based quantum dot coated with PEG6000 [PEG-TA-AuQDs]

The TEM images and size distribution of AuQDs and PEG-TA-AuQDs are shown in Fig. 1a–d. The HR-TEM image and d-spacing of the PEG-TA-AuQDs are shown in Fig. 1e and f. The TEM image of PEG-TA-AuQDs (tannic acid-based AuQDs with PEG 6000) indicated that these nanoparticles exhibited spherical shape and homogeneous distribution of the PEG matrix. The size distribution analysis showed that the diameter of PEG-TA-AuQDs ranged from 2 to 5 nm. To further characterize PEG-TA-AuQDs, HR-TEM was performed, which revealed fringes on the surface of

the spherical gold nanoparticles. The observed d-spacing to be 0.24 nm. These results suggest that tannic acid acted as a potential reducing and stabilizing agent in the formation of spherical PEG-TA-AuQDs (Fig. 1).

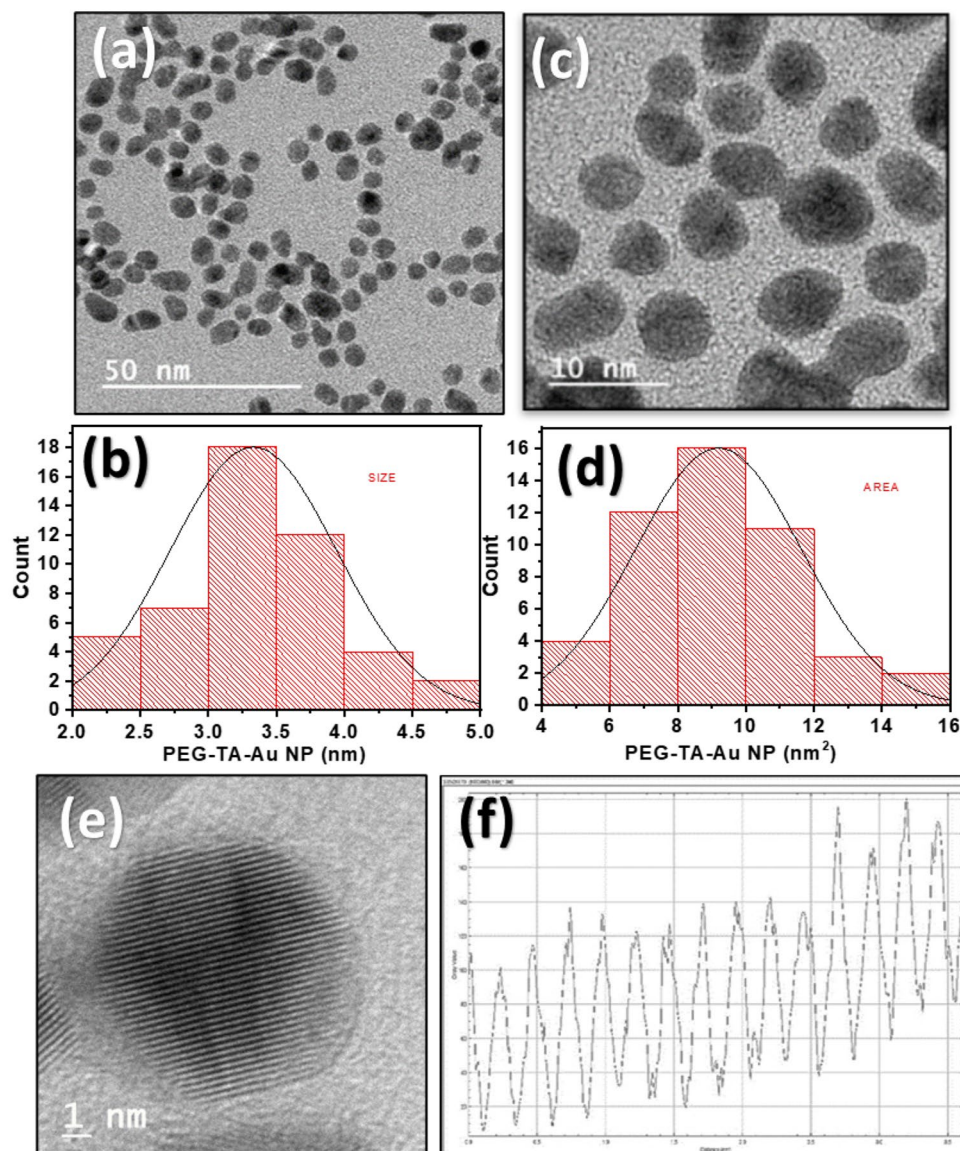
3.2 Morphological properties of FA-PEG-TA-AuQDs [folic acid attached to PEG-TA-AuQDs]

After using the EDC/NHS coupling reaction, folic acid was attached and TEM was carried out, and depicted in Fig. 2. It is showing in increase of size from 2 to 5 nm to 9 to 10 nm, indicating successful attachment of folic acid to PEG-TA-AuQDs.

3.3 XPS studies

The elemental composition and its oxidation states were analyzed by high resolution X-ray photoelectron spectroscopy. Figure 3 shows the XPS spectra of PEG-TA-AuQDs. Figure 3a represents the hyperfine splitting of calcium 2p orbitals. The orbital states Ca 2p_{3/2} and Ca 2p_{1/2} were further split in three states having oxidation states 0, +1, and +2 having corresponding binding energies 345.97, 346.66, and 347.45 eV for Ca 2p_{3/2} state and 349.45, 349.96, and 350.75 eV, respectively. The energy differences between similar oxidation states of Ca2p_{3/2} and Ca2p_{1/2} are nearly 3.3 eV [27]. Figure 3b C1s spectrum, the splitting gives the three components assigned to C–C, C–O–CH, and O=C=C with respective binding energy 284.19, 286, and 287.32 eV. Figure 3c shows the sodium 1s spectra, since there is

Fig. 1 TEM images. **a, c** Histogram of size distribution; **b, d** HR-TEM image; **e** Graph of d-spacing; **f** PEG-TA-AuQDs



single unpaired electron in 3s orbital it has only single X-ray peak which is assigned to Na metal with binding energy 1071.33 eV.

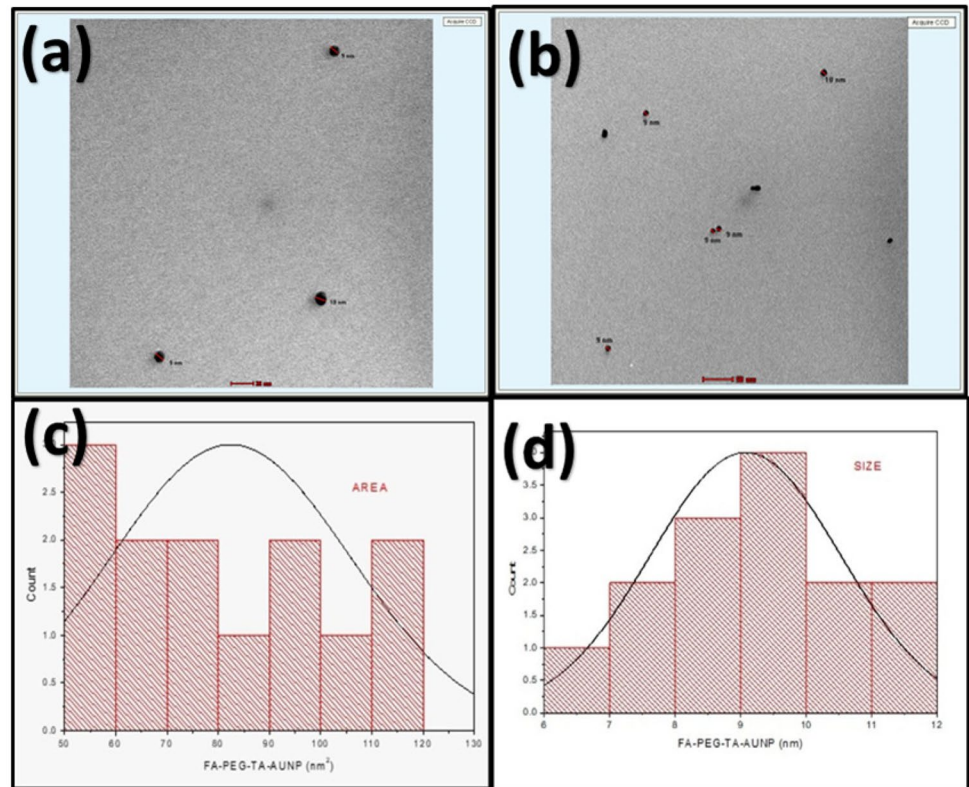
Figure 3d represents the O1s spectra and the peaks in O1s correspond to chemical species, C–O–H and C=O having binding energy 530.27, 531.66, and 532.44 eV, respectively [28, 29]. The FWHM and relative peak intensities are represented in Tables 1–3 of the supporting information.

Figure 4 represents the XPS spectra of 5FU-attached FA-PEG-TA-AuQDs. Figure 4a represents C1s spectrum having splitting components C–C/C–H, C–N/C–O and C=O having binding energy as 283.75,

285.37, and 287.21 eV, respectively. Figure 4b represents hyperfine splitting of Au 4f orbital having $4f_{7/2}$ and $4f_{5/2}$ sub-orbitals. The oxidation states for $4f_{7/2}$ orbital are 0, +1, and +3 having binding energies 82.66, 83.4, and 86.07 eV, while the same for $4f_{5/2}$ orbital are 0, +1, and +3 with binding energies 86.58, 87.75, and 89 eV, respectively. Au 4f region has well-separated spin orbit components $\Delta = 3.92$ eV with peaks having asymmetric shape [30].

Figure 4c gives the XPS spectra of F 1s, with metal-F peaks at 685.89 eV and org. F having binding energy at 686.55 eV. Also, Fig. 4d represents the N 1s peak with 1s splitting ascribed to C–N=C and C–NH=C having corresponding binding energy

Fig. 2 TEM images (a, b) and histogram (c, d) of FA-PEG-TA-AuQDs



as 397.5, and 399.19 eV. Also, peak position for Na 1 s orbital remains unaltered with binding energy 1071.33 eV as represented in Fig. 4e. Metal–Oxide and metal–carbon peaks O 1 s have binding energies at 530.33 and 5.31.63 eV. The C=O chemical bonding with binding energy 532.34 eV is observed on O1s spectra [29, 31]. The FWHM and relative peak intensities are represented in Tables 4–8 of the supporting information. These data confirm the conjugation and spectrum of elements present in each sample.

3.4 FTIR study

FTIR spectral analysis of 5FU-attached FA-PEG-TA-Au QDs was performed (Fig. 5) to describe chemical conjugation of PEG and TA-Au QDs [32]. Spectral graphs were compared to standard spectral graph of PEG binding to gold nanoparticles [33] to determine whether the spectrum showed conjugation or the presence of PEG [34]. Frequencies observed at 960.18 and 841.63 cm⁻¹.

indicated successful binding of PEG to nanoparticles when compared to standardize graph of PEG attached to gold nanoparticle giving the vibration peaks of C=C [35]. Due to presence of above functional groups and their comparisons by standard graphs, the

binding of PEG with to the gold quantum dots is successfully observed.

UV–Vis absorption spectra of 5-FU solutions of different concentrations after being loaded in a GO dispersion (8 mg mL).

3.5 Spectra of UV–vis absorption of FA-polymer-AuQDs nano-conjugates

The UV–vis absorption spectrum of the gold quantum dots (AuQDs) and drug-loaded nanoconjugate displayed two absorption bands at 537 and 531 nm (Fig. 6). The former is believed to originate from the surface plasmon absorption of AuQDs, which is present in both the FA-PEG-TA-AuQDs and the nanoparticle solution, with a peak shift of 4.92 nm. The location of the band for AuQDs is predominantly influenced by the size of the Au particles and hence the absorption position of this peak serves as an indicator that the AuQDs are very small in size. This assumption was further supported by transmission electron microscopy (TEM) analysis. TEM analysis

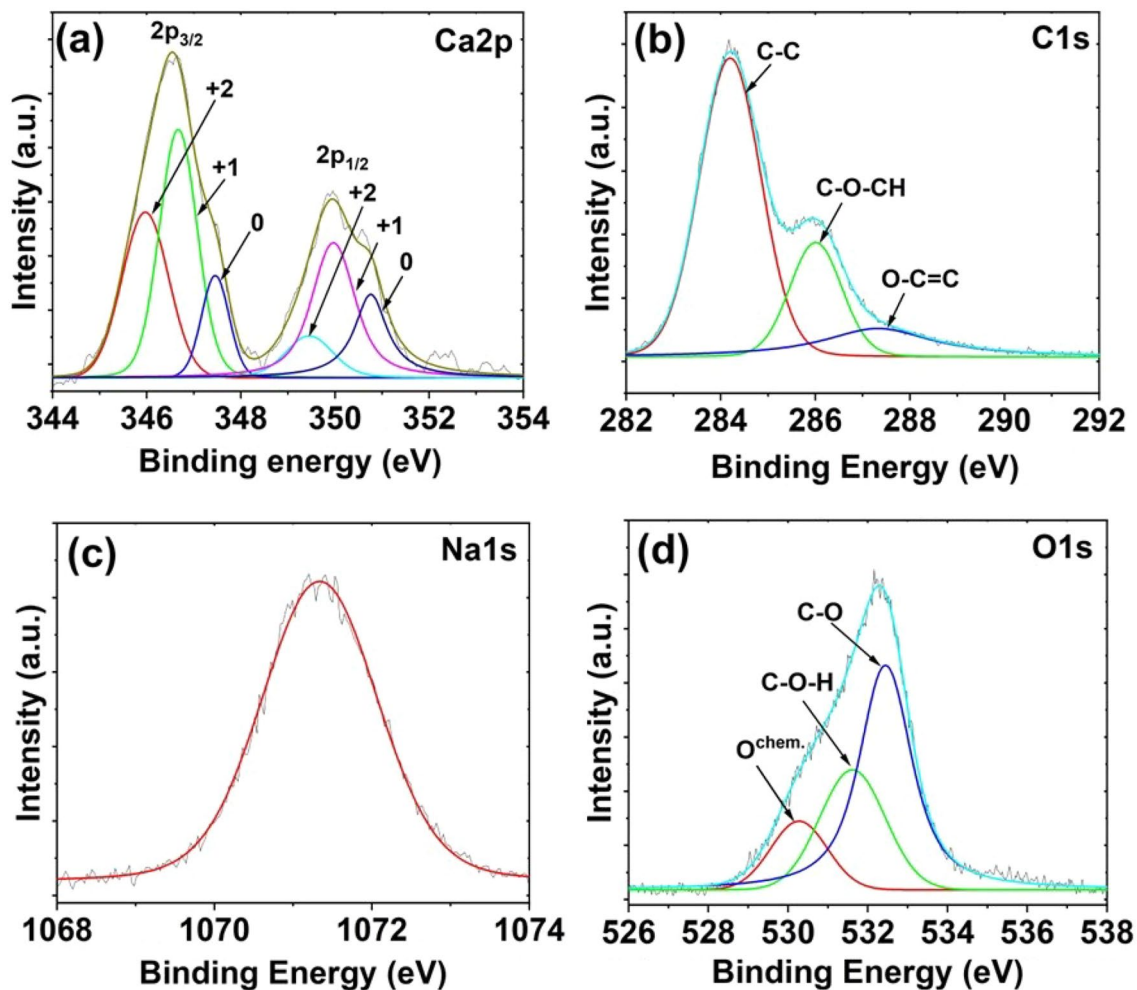


Fig. 3 X-ray photoelectron spectroscopy (XPS) spectra of PEG-TA-AuQDs. **a–d** Graphs of respective elements recorded by XPS

revealed that the AuQDs are indeed very small, with an average diameter of only 3.7 nm. The particles were mostly spherical in shape and well dispersed in the solution. The images also showed that the 5FU drug was present in the nanoparticle solution, confirming the results obtained from the UV–vis absorption spectrum. In conclusion, the UV–vis absorption spectrum of the AuQDs and solution showed the presence of the surface plasmon absorption of AuQDs, indicating the small size of the particles. TEM analysis further confirmed the small size of the particles and the presence of the PEG in the nanoparticle solution.

4 Conclusion

In conclusion, this study successfully synthesized FA-functionalized, tannic acid-based gold quantum dots. Tannic acid played a dual role as a reducing agent and a stabilizing agent. The use of PEG6000 as a coating agent increased the carrying capacity and stability of the nanoparticles. FTIR data confirmed the presence of polymer-AuQDs and 5FU loading on nanoconjugates after attachment to FA. XPS results revealed that tannic acid and PEG 6000 were conjugated, and the samples contained O, C, Cl, K, and Na. This study may provide a practical framework for the preparation of FA-functionalized, tannic acid-based gold quantum dots which can be potentially used in various medical applications, which could have significant implications in the biomedical field.

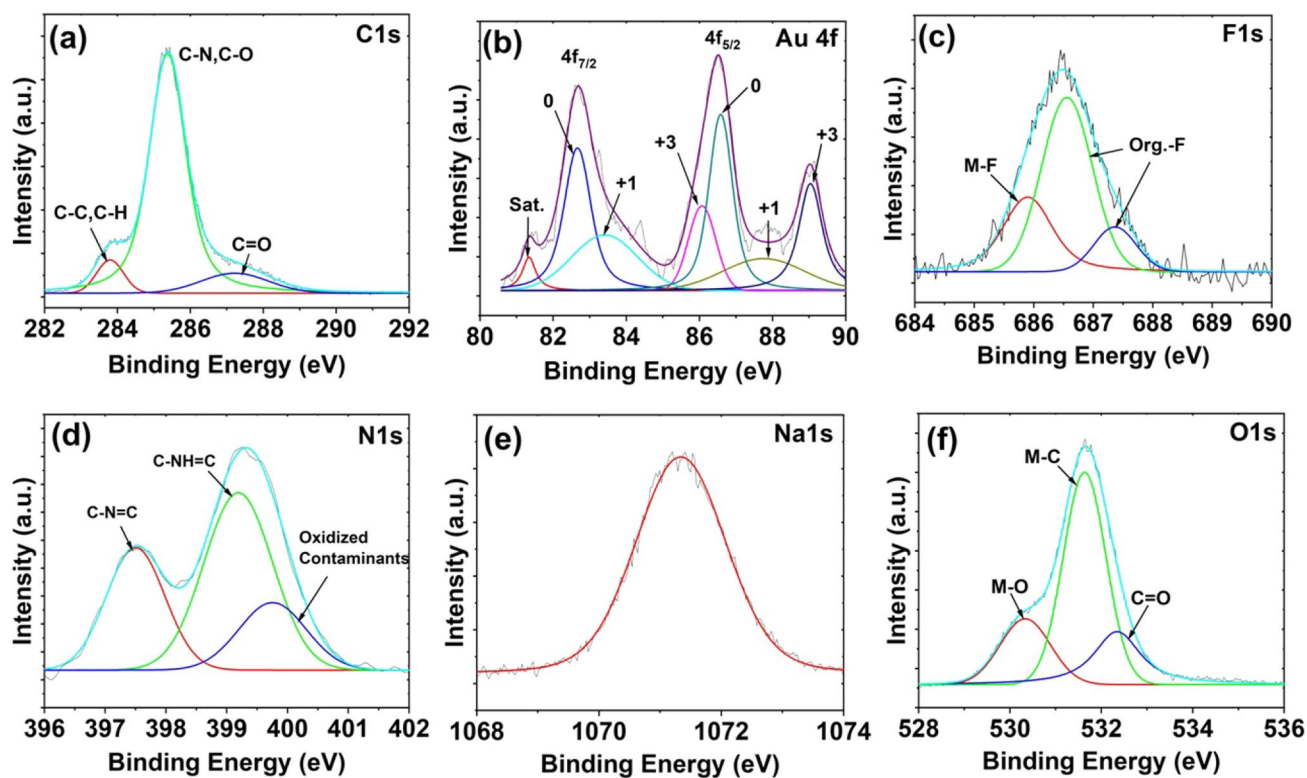


Fig. 4 X-ray photoelectron spectroscopy (XPS) spectra of 5FU attached FA-PEG-TA-Au QDs. **a–f** Graphs of respective elements recorded by XPS

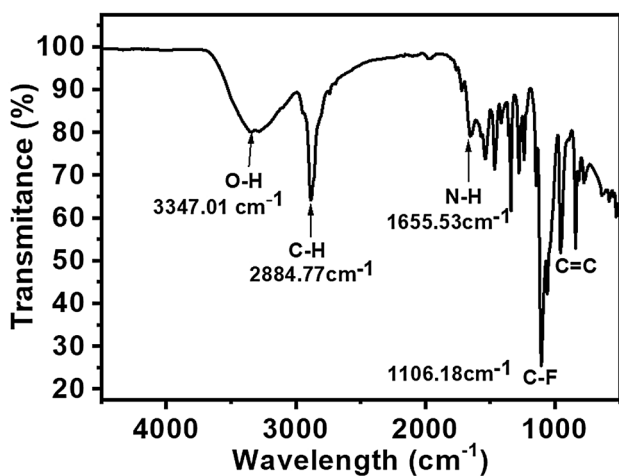


Fig. 5 FTIR spectral analysis of PEG attached FA-PEG-TA-AuQDs

Acknowledgements

The authors are thankful to Rashtriya Uchchar Shiksha Abhiyan, Ministry of Education, Government of India for financial support, carried out

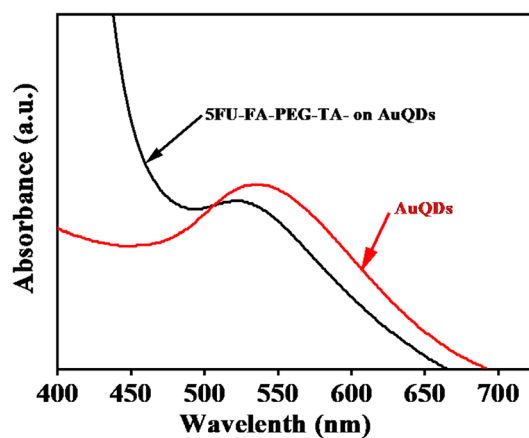


Fig. 6 UV–VIS absorption of FA-PEG-TA-AuQDs and AuQDs

at Rayat Shikshan Sanstha's Karmaveer Bhaurao Patil College Vashi, Navi Mumbai. Additionally, this work was supported by a grant of the National Research Foundation of Korea (NRF) Grant funded by the Korea government (MSIT, NRF-2022R1A4A1032832).

Author contributions

KJC contributed to data curation, and Formal analysis, SRB: contributed to investigation and writing of the original draft, GMG contributed to data curation and conceptualization, BMP contributed to formal analysis and editing of the original draft, TK contributed to data curation and Methodology, HK contributed to investigation and data curation, APT contributed to formal analysis and editing the draft, II contributed to conceptualization and supervision, RNB contributed to conceptualization, editing the draft, and Supervision, JMK contributed to conceptualization, funding acquisition, project administration, and supervision.

Funding

This study was supported by Ministry of Science and ICT, South Korea, NRF-2022R1A4A1032832.

Data availability

Data will be made available on reasonable request.

Declarations

Conflict of interest The authors declare that they have no conflicts of interest.

Supplementary Information The online version contains supplementary material available at <https://doi.org/10.1007/s10854-023-11489-1>.

References

1. X. Tang, W.S. Loc, C. Dong, G.L. Matters, P.J. Butler, M. Kester, C. Meyers, Y. Jiang, J.H. Adair, The use of nanoparticles to treat breast cancer. *Nanomedicine* **12**(19), 2367–2388 (2017). <https://doi.org/10.2217/nmm-2017-0202>
2. K.P. Seremeta, D.A. Chiappetta, A. Sosnik, Poly (ϵ -caprolactone), Eudragit® RS 100 and poly (ϵ -caprolactone)/Eudragit® RS 100 blend submicron particles for the sustained release of the antiretroviral efavirenz. *Colloids Surf. B* **102**, 441–449 (2013). <https://doi.org/10.1016/j.colsurfb.2012.06.038>
3. H.S. Zavareh, M. Pourmadadi, A. Moradi, F. Yazdian, M. Omid, Chitosan/carbon quantum dot/apramer complex as a potential anticancer drug delivery system towards the release of 5-fluorouracil. *Int. J. Biol. Macromol.* **165**, 1422–1430 (2020). <https://doi.org/10.1016/j.ijbiomac.2020.09.166>
4. L. Nair, S. Jagadeeshan, S.A. Nair, G.V. Kumar, Biological evaluation of 5-fluorouracil nanoparticles for cancer chemotherapy and its dependence on the carrier, PLGA. *Int. J. Nanomed.* **6**, 1685–1697 (2011). <https://doi.org/10.2147/IJN.S20165>
5. M.A. Safwat, G.M. Soliman, D. Sayed, M.A. Attia, Gold nanoparticles enhance 5-fluorouracil anticancer efficacy against colorectal cancer cells. *Int. J. Pharm.* **513**(1–2), 648–658 (2016). <https://doi.org/10.1016/j.ijpharm.2016.09.076>
6. J. Conde, G. Doria, P. Baptista, Noble metal nanoparticles applications in cancer. *J. Drug Deliv.* **2012**, 1–12 (2012). <https://doi.org/10.1155/2012/751075>
7. B. Bahrami, M. Mohammadnia-Afrouzi, P. Bakhshaei, Y. Yazdani, G. Ghalamfarsa, M. Yousefi, S. Sadreddini, F. Jadidi-Niaragh, M. Hojjat-Farsangi, Folate-conjugated nanoparticles as a potent therapeutic approach in targeted cancer therapy. *Tumor Biol.* **36**, 5727–5742 (2015). <https://doi.org/10.1007/s13277-015-3706-6>
8. A. Shakeri-Zadeh, M. Ghasemifard, G. Ali Mansoori, Structural and optical characterization of folate-conjugated gold-nanoparticles. *Phys. E Low-Dimens. Syst. Nanostruct.* **42**(5), 1572–1280 (2010). <https://doi.org/10.1016/j.physe.2009.10.039>
9. L. Papaioannou, A. Angelopoulou, S. Hatziantoniou, M. Papadimitriou, P. Apostolou, I. Papatotiriou, K. Avgoustakis, Folic acid-functionalized gold nanorods for controlled paclitaxel delivery: in vitro evaluation and cell studies. *AAPS PharmSciTech* **20**, 1–13 (2019). <https://doi.org/10.1208/s12249-018-1226-6>
10. J. Singh, T. Dutta, K.-H. Kim, M. Rawat, P. Samddar, P. Kumar, ‘Green’ synthesis of metals and their oxide nanoparticles: applications for environmental remediation. *J. Nanobiotechnol.* **16**(1), 1–24 (2018). <https://doi.org/10.1186/s12951-018-0408-4>
11. Y. Han, J. Zhou, Y. Hu, Z. Lin, Y. Ma, J.J. Richardson, F. Caruso, Polyphenol-based nanoparticles for intracellular protein delivery via competing supramolecular interactions. *ACS Nano* **14**(10), 12972–12981 (2020). <https://doi.org/10.1021/acsnano.0c04197>
12. K.T. Shimizu, W.K. Woo, B.R. Fisher, H.J. Eisler, M.G. Bawendi, Surface-enhanced emission from single semiconductor nanocrystals. *Phys. Rev. Lett.* **89**, 117401 (2002). <https://doi.org/10.1103/PhysRevLett.89.117401>

13. Y. Wang, J.E.Q. Quinsaat, T. Ono, M. Maeki, M. Tokeshi, T. Isono, K. Tajima, T. Satoh, S. Sato, Y. Miura, T. Yamamoto, Enhanced dispersion stability of gold nanoparticles by the physisorption of cyclic poly(Ethylene Glycol). *Nat. Commun.* **11**(1), 6089 (2020). <https://doi.org/10.1038/s41467-020-19947-8>
14. L. Shi, J. Zhang, M. Zhao, S. Tang, X. Cheng, W. Zhang, W. Li, X. Liu, H. Peng, Q. Wang, Effects of polyethylene glycol on the surface of nanoparticles for targeted drug delivery. *Nanoscale* **13**, 10748–10764 (2021). <https://doi.org/10.1039/D1NR02065J>
15. D. Ren, F. Kratz, S.-W. Wang, Engineered drug-protein nanoparticle complexes for folate receptor targeting. *Biochem. Eng. J.* **89**, 33–41 (2014). <https://doi.org/10.1016/j.bej.2013.09.008>
16. D. Ioannou, D.K. Griffin, Nanotechnology and molecular cytogenetics: the future has not yet arrived. *Nano Rev.* **1**, 5117 (2010). <https://doi.org/10.3402/nano.v1i0.5117>
17. A. Youness, R. Kamel, R.A. Elkasabgy, N. Shao, P.A. Farag, Recent advances in tannic acid (Gallotannin) anti-cancer activities and drug delivery systems for efficacy improvement; a comprehensive review. *Molecules* **26**, 1486 (2021). <https://doi.org/10.3390/molecules26051486>
18. S.S. Chauhan, A.B. Shetty, E. Hatami, P. Chowdhury, M.M. Yallapu, Pectin-tannic acid nano-complexes promote the delivery and bioactivity of drugs in pancreatic cancer cells. *Pharmaceutics* **12**, 285 (2020). <https://doi.org/10.3390/pharmaceutics12030285>
19. W.C.W. Chan, S. Nie, Quantum dot bioconjugates for ultrasensitive nonisotopic detection. *Science* **281**, 2016–2018 (1998). <https://doi.org/10.1126/science.281.5385.2016>
20. M. Bruchez, M. Moronne, P. Gin, S. Weiss, A.P. Alivisatos, Semiconductor nanocrystals as fluorescent biological labels. *Science* **281**, 2013–2016 (1998). <https://doi.org/10.1126/science.281.5385.2013>
21. P. Chowdhury, P.K.B. Nagesh, E. Hatami, S. Wagh, N. Dan, M.K. Tripathi, S. Khan, B.B. Hafeez, B. Meibohm, S.C. Chauhan, M. Jaggi, M.M. Yallapu, Tannic acid-inspired paclitaxel nanoparticles for enhanced anticancer effects in breast cancer cells. *J. Colloid Interface Sci.* **535**, 133–148 (2019). <https://doi.org/10.1016/j.jcis.2018.09.072>
22. W. Russ Algar, M. Massey, U.J. Krull, The application of quantum dots, gold nanoparticles and molecular switches to optical nucleic-acid diagnostics. *TrAC Trends Anal. Chem.* **28**, 292–306 (2009). <https://doi.org/10.1016/j.trac.2008.11.012>
23. J. Kimling, M. Maier, B. Okenve, V. Kotaidis, H. Ballot, A. Plech, Turkevich method for gold nanoparticle synthesis revisited. *J. Phys. Chem. B* **110**(32), 15700–15707 (2006). <https://doi.org/10.1021/jp061667w>
24. J. Piella, N.G. Bastús, V. Puntes, Size-controlled synthesis of sub-10 nm citrate-stabilized gold nanoparticles and related optical properties. *Chem. Mater.* **28**(4), 1066–1075 (2016). <https://doi.org/10.1021/acs.chemmater.5b04406>
25. K. Ranaszek-Soliwoda, E. Tomaszewska, E. Socha, P. Krzyczmonik, A. Ignaczak, P. Orłowski, M. Krzyzowska, G. Celichowski, J. Grobelny, The role of tannic acid and sodium citrate in the synthesis of silver nanoparticles. *J. Nanopart. Res.* **19**, 273 (2017). <https://doi.org/10.1007/s11051-017-3973-9>
26. V. Amendola, M. Meneghetti, Size evaluation of gold nanoparticles by UV–vis spectroscopy. *J. Phys. Chem. C* **113**(11), 4277–4285 (2009). <https://doi.org/10.1021/jp8082425>
27. A. Al-Mamoori, S. Lawson, A.A. Rownaghi, F. Rezaei, Improving adsorptive performance of CaO for high-temperature CO₂ capture through Fe and Ga doping. *Energy Fuels* **33**, 1404–1413 (2019). <https://doi.org/10.1021/acs.energyfuels.8b03996>
28. M. Tou, R. Michalsky, A. Steinfeld, Solar-driven thermochemical splitting of CO(2) and in situ separation of CO and O(2) across a ceria redox membrane reactor. *Joule* **1**(1), 146–154 (2017). <https://doi.org/10.1016/j.joule.2017.07.015>
29. N. Nakatsuka, M.M. Hasani-Sadrabadi, K.M. Cheung, T.D. Young, G. Bahlakeh, A. Moshaverinia, P.S. Weiss, A.M. Andrews, Polyserotonin nanoparticles as multifunctional materials for biomedical applications. *ACS Nano* **12**(5), 4761–4774 (2018). <https://doi.org/10.1021/acsnano.8b01470>
30. M. Nazemi, L. Soule, M. Liu, M.A. El-Sayed, Ambient ammonia electrosynthesis from nitrogen and water by incorporating palladium in bimetallic gold-silver nanocages. *J. Electrochem. Soc.* **167**, 054511 (2020). <https://doi.org/10.1149/1945-7111/ab6ee9>
31. M. Todea, M. Muresan-Pop, S. Simon, C. Moiescu-Goia, V. Simon, D. Eniu, XPS investigation of new solid forms of 5-fluorouracil with piperazine. *J. Mol. Struct.* **1165**, 120–125 (2018). <https://doi.org/10.1016/j.molstruc.2018.03.122>
32. D.C. Manatunga, R.M. de Silva, K. de Silva, D.T. Wijeratne, G.N. Malavige, G. Williams, Fabrication of 6-gingerol, doxorubicin and alginate hydroxyapatite into a biocompatible formulation: enhanced anti-proliferative effect on breast and liver cancer cells. *Chem. Cent. J.* **12**(1), 1–13 (2018). <https://doi.org/10.1186/s13065-018-0482-6>

33. P. Priya, A. Raja, V. Raj, Interpenetrating polymeric networks of chitosan and egg white with dual crosslinking agents polyethylene glycol/polyvinylpyrrolidone as a novel drug carrier. *Cellulose* **23**, 699–712 (2016). <https://doi.org/10.1007/s10570-015-0821-x>
34. O. Merve, N. Şanlı, E. Kondolot Solak, Release of anticancer drug 5 fluorouracil from different ionically crosslinked alginate beads. *J. Biomater. Nanobiotechnol.* **3**(4), 469–479 (2012). <https://doi.org/10.4236/jbnb.2012.34048>
35. A. Reddy Polu, R. Kumar, Impedance spectroscopy and FTIR studies of PEG-based polymer electrolytes. *E-J. Chem.* **8**(1), 347–353 (2011). <https://doi.org/10.1155/2011/628790>

Publisher's Note Springer Nature remains neutral with regard to jurisdictional claims in published maps and institutional affiliations.

Springer Nature or its licensor (e.g. a society or other partner) holds exclusive rights to this article under a publishing agreement with the author(s) or other rightsholder(s); author self-archiving of the accepted manuscript version of this article is solely governed by the terms of such publishing agreement and applicable law.